Universidade de Lisboa

Faculdade de Farmácia

Investigating Electrospinning to Prepare Nanofibers Suitable for Neurological Disorders

Rita Candeias Ramos

Mestrado Integrado em Ciências Farmacêuticas

2020

Universidade de Lisboa

Faculdade de Farmácia

Investigating Electrospinning to Prepare Nanofibers Suitable for Neurological Disorders

Rita Candeias Ramos

Monografia de Mestrado Integrado em Ciências Farmacêuticas apresentada à Universidade de Lisboa através da Faculdade de Farmácia

Orientadora: Professora Associada na University College London School of Pharmacy, Doutora Asma Buanz

Co-Orientadora: Professora Associada, Doutora Maria Henriques Lourenço Ribeiro

2020

Resumo

O presente estudo tem como objetivo investigar o *electrospinning* como sistema de veiculação de fármacos no tratamento da epilepsia. As fibras fabricadas por electrospinning serão compostas por um fármaco, a carbamazepina (CBZ), e um polímero, o poli(ácido lático-co-ácido glicólico) (PLGA). Os fenómenos térmicos observados por varredura diferencial de calorimetria (DSC) permitiram a interpretação do comportamento do fármaco e do polímero, em diferentes misturas. Como previsto pelas análises molecular e cristalográfica, as duas moléculas não têm tendência para interagir em mistura, e a carbamazepina tende a permanecer sob forma cristalina. Os resultados de DSC poderão significar uma maior estabilidade a longo prazo devido ao seu conteúdo cristalino, hipótese que deverá ser testada. As várias fibras e partículas foram analisadas por microscopia SEM e os parâmetros foram ajustados de forma a obter fibras uniformes de PLGA. Concluiu-se que não só o peso molecular de PLGA, como também a escolha de solvente influencia a formação de nanofibras em virtude de nanopartículas. As fibras de PLGA foram fabricadas com sucesso e os parâmetros ideais para fibras uniformes foram estabelecidos. Estudos morfológicos demonstraram que a capacidade de *electrospinning* do PLGA aumentou com o aumento do seu peso molecular e que a escolha do solvente influenciou a formação das fibras devido aos seus efeitos nas propriedades reológicas. A análise por DSC das fibras de PLGA demonstrou ser semelhante à análise inicial de PLGA. No entanto, tal não garante um comportamento semelhante entre as misturas de CBZ e PLGA, e as fibras de PLGA com CBZ, pelo que devem continuar a investigar-se o comportamento das fibras com CBZ. O presente estudo demonstra um potencial para o fabrico de fibras de CBZ-PLGA, mas o seu comportamento exato necessita de mais investigação.

Palavras-Chave: Epilepsia, Electrospinning, Nanofibras, Carbamazepina, PLGA

Abstract

The aim of this work was to investigate electrospinning for fabrication of anti-epileptic drug fibers intended for surgical implantation in selected epilepsy patients. Electrospun fibers can potentially be a good alternative to current therapies available, allowing fabrication of coaxial fibers that join chemical and genetic-based therapeutics. Carbamazepine (CBZ) was the selected drug because of its vast therapeutic usage and high efficacy. Thermal analysis with differential scanning calorimetry (DSC) showed that CBZ and PLGA (polylactic-co-glycolic acid), the selected polymer, did not interact and, instead, carbamazepine remained crystalline. This was confirmed by crystal structure data analysis of different carbamazepine forms. However, this data hint that the formulation could be more stable long-term, due to its crystalline content. PLGA fibers were successfully fabricated and ideal parameters for uniform fibers under SEM were established. Morphology studies showed that PLGA electrospinnability increased as its grade also increased, and that the choice of solvent influenced the formation of the fibers due to its effects on rheological properties. The final electrospun PLGA-only fibers DSC analysis showed similar thermal behavior to plain PLGA's, however, this does not guarantee same behavior from CBZ-PLGA mixtures and CBZ-loaded fibers. The present study demonstrated the potential of CBZ-PLGA fibers, but the exact behavior of the electrospun fibers requires further research.

Keywords: Epilepsy, Electrospinning, Nanofibers, Carbamazepine, PLGA

Acknowledgments

Abbreviations

AED	Anti-Epileptic Drug
ASD	Amorphous Solid Dispersion
BBB	Blood-Brain Barrier
BFDH	Bravais, Friedel, Donnay and Harker
CBZ	Carbamazepine
CCDC	Cambridge Crystallographic Data Centre
CSD	Cambridge Structural Database
DCM	Dichloromethane
DMF	Dimethylformamide
DSC	Differential Scanning Calorimetry
EMA	European Medicines Agency
FDA	Food and Drug Administration
HPC	Hydroxypropylcellulose
HPMC	Hydroxypropylmethyl Cellulose
PEG	Polyethylene Glycol
PLGA	Polylactic-co-glycolic Acid
PVA	Polyvinyl Alcohol
PVP	Polyvinylpyrrolidone
SEM	Scanning Electron Microscopy
Tg	Glass Transition Temperature

Content

List of Figures

List of Tables

1. Introduction

The main aim of the present study is to generate coaxial electrospun nanofibers for surgical application in selected Epilepsy patients. The fibers will be composed of anti-epilepsy drugs and a specific gene, aimed for co-delivery in the brain of selected patients. Merging both chemical and gene therapies was proven to be successful in the treatment of cancer with significant progresses being made in the efficacy, due to their synergistic effect[1]. This new finding opens new routes for the strategic development of systems to improve treatment of cancer as well as other pathologies, through the synergetic effect of chemical and gene therapy. For this project, we aim to apply this novel strategy towards epilepsy therapy. So, the global intent is to generate coaxial electrospun nanofibers, in which the core is loaded by a specific gene and the shell is loaded with anti-epileptic drug.

In the present project, we report the formation of drug-loaded nanofibers that will compose the outer layer of the coaxial fibers by electrospinning. This report will focus on the pre-formulation and formulation stages of nanofibers of anti-epileptic drug loaded polymer. For this, theoretical aspects related to the disease will firstly be discussed. Then, a summary on the selected drug, carbamazepine, and its solubility and stability challenges will be presented; followed by an electrospinning technique overview.

1.1. Epilepsy

Epilepsy is defined as a chronic brain disease that affects over 70 million people worldwide, characterized by unprovoked seizures[2,3]. Although its diagnostic is still complex, as seizures can be multifactorial[4], the consent diagnostic criteria is defined as: two unprovoked seizures occurring more than 24 hours apart; a single unprovoked seizure if the recurrence risk is high; or a diagnosis of an epilepsy syndrome[5]. Epilepsy is considered one of the most serious brain pathologies, comprising neurobiological, cognitive, and psychosocial consequences, including loss of awareness and possibly even death[2,3]. Specialists agree that it should be one of the global health's priority, especially since there are cost-effective treatments in the market that could minimize morbidity and mortality[3].

Approximately 70% of these patients are adequately controlled with oral anti-epileptic drugs (AEDs), while the remaining 30% are unresponsive to oral therapy. It was observed that although the antiepileptic drug plasma concentration in the latter group of patients is within normal therapeutic values, they appear to be pharmacoresistent. Studies have pointed out that changes in the permeability of AEDs across the blood-brain barrier (BBB) may be a big factor involved in pharmacoresistance[6].

Moreover, the latter group could benefit from new approaches, via surgical intervention. Resective surgery has been used but its success rate highly depends on the affected brain site. Data from previous studies suggest that temporal lobe surgery has a reasonably high rate of seizure relief (55% to 70%), while only 30% to 50% of individuals undergoing extratemporal resection become totally seizure free[7,8]. Moreover, areas of resection near the vital cortex are related to higher complication risks, regarding language, motor complications or sensory

functions loss. This type of surgery requires careful risk-benefit analysis, and it is often unsuitable for seizure focus in deeper brain regions[2,7,8]. Novel local treatments such as neurostimulation techniques and on-site drug delivery systems have emerged as better alternatives[2,4,9]. Local drug delivery to the brain's area in which seizures are originated is a promising approach, allowing a high concentration of drug to be available at the target site. They show great effectiveness while reducing side effects inherent to systemic treatments[2,9]. Implantable devices could be fabricated by 3D printing, electrospraying or electrospinning, and have been showing potential for on-site delivery in the brain[2].

Additionally, combining gene therapy with pharmaceutical therapy is an favorable method, already studied for cancer treatment[1]. It was proven that merging both pharmacological and gene therapies was successful due to their apparent synergistic effect. In epilepsy, gene therapy is still experimental[3], but researchers believe that it can hold the potential for cure[10]; while pharmacological options, such as carbamazepine, phenytoin, gabapentin, are widely used. So, it would be interesting to explore the possible synergetic effect between an anti-epileptic drug and a gene therapy for epilepsy.

Oral drugs present some disadvantages like the lack of responsiveness in 30% of the patients, side effects, toxicity, and possible failure to cross the blood-brain barrier (BBB)[11]. Nevertheless, amongst used drugs, carbamazepine remains the top choice for its effectiveness, safety and favorable economic issues[12].

1.2. Carbamazepine

Carbamazepine (5H-dibenzo[b,f]azepine-5-carboxamide) is one of the most commonly used antiepileptic drugs. Its antiepileptic effect was first reported by Theobald and Kunz (1963)[13] and later utilized as an antiepileptic drug (AED) in Europe since 1965[11]. The ring structure has structural features of the tricyclic antidepressants. Despite this structural similarity, effects and mechanism of action differ significantly. Carbamazepine (CBZ) is a white or almost white crystalline powder and a first-generation anticonvulsant drug that has been used to treat partial seizures, trigeminal neuralgia, manic-depressive illness, and explosive aggression for nearly 40 years[14].

Its mechanism of action is not well understood, although some evidence suggests that it binds mainly to voltage-dependent sodium channels in some regions of the brain, blocking them. This suppresses the progress of the action potential and inhibits the forwarding of information. Interactions with calcium and potassium channels have also been reported before. Moreover, carbamazepine increases the inhibitory effect of GABA and cuts the excitatory effect of glutamate. Due to the influence on different ion channels, it is currently assumed that carbamazepine acts by stabilizing the resting membrane potential and inhibiting synaptic transmission. This reduces repetitive neural discharges and reduces the spread of synaptic excitation[11,13].

Carbamazepine had the best result in cooperative US Department of Veterans Affairs study, showing to have the top balance of efficacy and tolerability[15]. No other drugs have been confirmed to be more effective than carbamazepine, but its use declined with the selling of new

AEDs, like lamotrigine, oxcarbazepine, and gabapentin, that showed pharmacokinetic advantages and had better tolerability than immediate release carbamazepine. Therefore, enzyme induction and pharmacokinetic interactions are issues that favor the use of newer AEDs, while economic issues favor the use of carbamazepine[12].

Four polymorphs of carbamazepine have been reported in the literature. They can be crystallized from different solvents. Among all of them, form III of carbamazepine is the most commonly used form in the commercialized tablets due to being the most stable one at room temperature and up to 78°C[14].

Regarding carbamazepine's pharmacokinetics, it is slowly absorbed after its oral administration and has a good bioavailability of about 75 to 85%. Its protein binding of about 75% is not of clinical importance; and it is mainly metabolized in the liver by CYP3A4, CYP3A5, and CYP2C8 enzymes. The elimination half-life of this drug is approximately 35 hours, but it is lower in children (approximately 10 hours) and higher in the elderly population (30 to 50 hours)[11,12].

Carbamazepine is classified as a class II drug in the Biopharmaceutics Classification System (BCS) because it has a low solubility (0.15 ± 0.07 mg/mL, 25°C) and a high permeability[16]. The transport of carbamazepine through BBB is mediated by many transporters (ABC efflux transporters, etc.) and it can be influenced by various drugs[6,17]. Its limited solubility in water has been a challenge in the development of pharmaceutical forms, as it is a rate-limiting step for absorption and bioavalilability[16,18].

1.3. Solubility & Stability Limitations

The two main factors to take into consideration while designing the carbamazepine nanofibers are drug solubility and stability. The first one, solubility, is an important physicochemical parameter affecting the whole process of drug discovery and development[19]. It is currently considered one of the biggest challenges that the pharmaceutical industry faces, especially with poorly water soluble drugs, like carbamazepine[20].

During the initial phases of drug discovery, the optimization process is aimed at maximizing the *in vivo* performance of the drug. Various techniques have been studied to enhance the dissolution rate and solubility of drugs, such as physical (particle reduction, dispersion in carriers, complexation and the use of surfactants), chemical etc.[16].

There are mainly two very successful methods to date that increase the solubility of the drug. The first one is the mechanical reduction of drug particle size, thereby increasing the surface area. Dissolution rate was shown to be dependent on surface area, as described by the Noyes-Whitney equation[21]. This equation indicates a direct relation between dissolution rate (dm/dt) and surface area (A). So, decreasing drug's size to nanoscale, thus increasing its surface area, allows a rise in the dissolution rate.

$$\frac{\mathrm{d}m}{\mathrm{d}t} = A\frac{D}{d}(C_s - C_b)$$

Where:
- dm/dt is the rate of dissolution
- A is the surface area
- D is the diffusion coefficient
- d is the diffusion layer thickness
- C_s is the particle surface (saturation) concentration
- C_b is the concentration in the bulk solvent/ solution

The second method used to increase drug solubility is the amorphization of the drug. Although crystalline forms have a higher stability as an advantage over amorphous forms, their lattice energy is a barrier to dissolution. Amorphous drug molecules' disorganized structure present higher free energy. This leads to higher dissolution rate, as well as apparent water solubility and oral absorption. However, pure amorphous molecules have little utility in pharmaceutical formulations due to their instability[21,22]. Instead, amorphous solid dispersions (ASD) have provided a novel alternative for overcoming solubility limitations, while showing higher stability and bioavailability[18,23]. Many methods can be utilized to form ASDs, one of them being electrospinning, which is reported as effective possibility in recent years. It uses electrical energy to induce changes from liquid to solid[22]. Nonetheless, for carbamazepine, it has been described that the reduction of size to the nanoscale is more significant than its amorphization[18].

1.4. Electrospinning

Electrospinning is a technology of increasingly interest worldwide. It can be defined as the formation of polymer nanofibers, from a polymeric solution that is injected through a nozzle under an electric field. It has recently gained the attention of scientists all over the world due to its vast versatility[2,24,25]. Interest in nanofibers rapidly increased in the last decade, with more than 1000 articles being published per year from 2014 to the present[26]. Fibers, instead of other structures, often present an increased mechanical performance, bigger flexibility, high surface-to-volume ratio, and malleability to conform to a wide variety shapes[24].

Electrospinning is a process to create nanofibers and microfibers spun from natural or synthetic polymers, drug-loaded polymers, nanoparticles-loaded polymers etc.[22,26–28]. It has potential for applications in diverse fields, including drug delivery[22,24,26,29], fibrous scaffolds and tissue engineering[24,30,31], and wound dressing[24,32]. It is somehow comparable to electrospraying, but it requires a more concentrated solution, a higher voltage and it results in the production of fibers instead of particles[33].

Apart from the normal electrospinning fibers, coaxial electrospinning has also been developed for controlled drug release of one or more substances. This is a process in which two layers of fibers are fabricated, and drugs, nanoparticles, or genes can be isolated in each layer[31,34,35].

Saraf *et al.*[31] have successfully used electrospinning to fabricate fibers loaded with a non-viral gene delivery vector and delivery plasmid DNA. Their intent was to incorporate those molecules in three-dimensional designed for tissue engineering, so that they could act as reservoirs[31]. For future stages of the present project, we aim to incorporate epilepsy gene therapy into electrospun coaxial fibers.

Core-shell nanofibers, as they are referred to, are very versatile in what concerns their types and sizes, and present some advantages over monolithic nanofibers, namely, improved drug stability and a greater control of the drug release profile. A great number of variable parameters can be tuned to control drug-release kinetics, drug encapsulation and drug stability. Nevertheless, core-shell electrospinning holds some unknown parameters, which can be challenging in nanofiber preparation and its reproducibility.[26]

The aim of the present study is to design and produce coaxial electrospun nanofibers composed of a core of gene-loaded polymer and a shell of drug-loaded polymer, targeting selected epilepsy patients. These nanofibers will be implanted in the brain, through brain surgery, in patients suffering from epilepsy who are unresponsive to oral therapy.

A variety of polymers have been used such as: naturally occurring polymers including hydroxypropylmethyl cellulose (HPMC), and hydroxypropylcellulose (HPC); and synthetic polymers such as polyvinylpyrrolidone (PVP), polyvinyl alcohol (PVA), and polyethylene glycol (PEG), and polylactic-co-glycolic acid (PLGA)[22].

1.5.   PLGA

Polylactic-co-glycolic acid (PLGA) is a biodegradable copolymer that is approved by both the US Food and Drug Administration (FDA) and the European Medicines Agency (EMA) for human application[36]. It is a copolymer prepared at different ratios of its constituent monomers, lactic acid (LA) and glycolic acid (GA)[37].

It is considered to have excellent biocompatibility since its hydrolysis results in breakage of its ester linkages and formation of lactate and glycolate, which are endogenous substances that can be incorporated in the Krebs cycle. Therefore, systemic toxicity post degradation is minimal. PLGA is one of the most successful carriers because of its favorable properties such as biodegradability, biocompatibility, regulatory agency approval, sustained release applications, ease of surface modification and capability to encapsulate both hydrophilic and hydrophobic drugs. Based on above properties, as a carrier it has wide applications in targeting, imaging, and diagnosis applications. Different ratios of LA to GA acid may exist as well as different molecular weight ranges, and the degradation time of the PLGA is dependent on both characteristics[28].

The functionality of electrospun fibers is highly dependent on choice of polymer because it affects the interactions between the API and the polymer, and overall fibers proprieties. For the past two decades, PLGA has been among the most attractive polymeric candidates used to fabricate devices for drug delivery and tissue engineering applications[38]. One of the relevant

parameters to be taken into consideration is the polymer's glass transition temperature (Tg). It is defined as the temperature at which a polymer changes from a glassy into a rubbery state, and it is associated with a characteristic small change in the heat capacity of the system[39]. In ASD forming methods, such as electrospinning, higher glass transition temperatures (Tg) are often preferable because they are associated with enhanced physical stability, due to lower the molecular mobility of the API.[22]

PLGA has successfully been incorporated in electrosprayed particles of different drugs; and been the polymer of choice for electrospun fibers for drug delivery, brain tissue, etc.[40]. In this study, electrospinning will be the method of choice to obtain carbamazepine-loaded nanofibers. Eventually, these will be the outer layer of coaxial fibers that will also include a gene-loaded layer. Here, pre-formulation aspects will be tested through thermal analysis, followed by analysis of the electrospun nanofibers of anti-epileptic drug.

2. Materials & Methods

2.1.   Materials

The materials utilized included PLGA (LA: GA, 75:25, molar ratio) polymer, with molecular weight of 17, 75-115, 90 and 154kDa. Carbamazepine polymorphic form III was used as the pharmaceutical drug. Carbamazepine was acquired from Sigma Aldrich (St Louis, MO, USA). 17, 90 and 154kDa PLGA samples were acquired from PURASORB® Corbion Purac (Gorinchem, the Netherlands). 75-115kDa PLGA was acquired from Alpha diagnostic Intl. Inc.

2.2.   Methods

2.2.1. Sample Preparation

- Physical mixtures preparation:

Suitable amounts of CBZ and PLGA were combined in DSC non-hermetic pans with aim to obtain physical mixtures with specific ratios: 9.0, 11.0, 12.5, 15.0, 20.0, 25.7, 30.0 and 50.0% w/w (drug in polymer).

- Electrospinning:

Fibers were produced utilizing an electrospinning setup SPRAYBASE® (Dublin, Ireland). The solution was transported and spun by a syringe pump at a flow rate of 0.6 mL/hr into a non-woven form nanofibrous membrane onto a collection plate at room temperature. The voltage was set to 10 kV, while the travel distance from the needle to the collection plate was 20 cm. The solvents used were acetone and dichloromethane: dimethylformamide (50:50).

2.2.2. Characterization

- Thermal analysis:

Differential scanning calorimetry (DSC) measurements were carried out in a TA Instruments Q2000 DSC using T_{zero} aluminum pans with lids. About 5 mg of samples was used for all the experiments, under dynamic nitrogen atmosphere of 50mL/min flow rate, at a heating rate of 10°C/min, and temperature range of 0–300°C. The pans used in all DSC measurements were non-hermetically sealed. The temperature and heat flow of the DSC instrument were calibrated with indium (melting point = 157.5 °C and DH = 26.7 J/g).

- Scanning Electron Microscopy (SEM):

The morphology and particle size of electrospun samples were imaged using a Quanta 200F field emission (FEG) SEM (FEI, the Netherlands).

2.3.   Extraction of Crystal Structure

Crystallographic data were calculated with the Bravais, Friedel, Donnay and Harker (BFDH) method, obtained in the *Mercury* Software. Mercury is a crystal structure visualization, analysis, design and prediction platform, developed at the Cambridge Crystallographic Data Centre (CCDC)[41]. The data set for the models was composed of the following molecules extracted from the Cambridge Structural Database (CSD): CBMZPN11, CBMZPN12 and CBMZPN22[42].

3. Results & Discussion

During the course of this study, pre-formulation aspects, namely, chemical structure, crystal analysis and carbamazepine-in-PLGA loading analysis were firstly addressed. Then, formulation of nanofibers by electrospinning followed, as well as and its morphological and thermal analysis.

Regarding carbamazepine loading analysis, different mixtures of carbamazepine-PLGA were melted and analysed in DSC, in different loadings. The loadings were chosen based on previous electrospraying or electrospinning studies with either PLGA or CBZ. The interpretation of the thermal data was intended to allow to understand how the mixture behaved thermally and to conclude which mixture was the most stable one. These first experiments were performed using PLGA grade 75-115kDa. Simultaneously, some electrospinning formulation studies began using various PLGA grades to fabricate nanofibers. Thus, similar thermal analysis with DSC, already performed for PLGA 75-115kDa, were repeated for PLGA grades 90kDa and 154kDa.

For formulation, ideal parameters for formation of PLGA fibers were tested: different PLGA grades, solvents, concentration of PLGA in solvent, equipment voltage and distance from needle to plate. The obtained PLGA fibers were, finally, subjected to DSC analysis.

3.1.   Chemical & Crystal Structure Data

Chemical structure of PLGA and carbamazepine, and crystal morphology of carbamazepine were analysed in the pre-formulation stage in order to predict possible interactions between both molecules.

Based on chemical structures, illustrated in Figures 1 and 2, interaction between the two molecules could be predicted through chemical reactions, namely, formation of hydrogen bonds. Carbamazepine has one hydrogen bond donor ($-NH_2$) and three hydrogen bond acceptors (2x C=O and N)[43]. PLGA can act as a hydrogen bond acceptor (HBA) via its carbonyl groups ($-C=O$) or as a hydrogen bond donor via its hydroxyl groups ($-OH$), that can act as both the hydrogen bond donor or acceptor[44]. Specifically, hydrogen bonds could be expected to form: i) between the carbonyl groups of PLGA and the amide group of CBZ (NH_2); ii) between the hydroxyl groups of PLGA and the amide group of carbamazepine (O or N as HBA); and iii) between the hydroxyl group of PLGA and the amide group of CBZ (NH_2) [44].
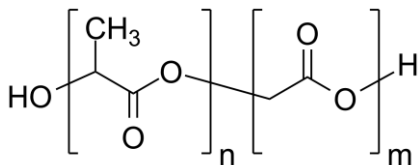
Figure 1 - PLGA Chemical Structure
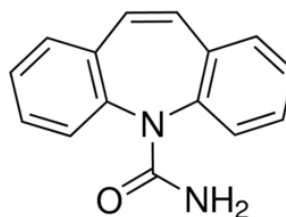
Figure 2 - Carbamazepine Chemical Structure

Crystal morphologies can be calculated with the Bravais, Friedel, Donnay and Harker (BFDH) method, which is based on d_{hkl} spacings of the crystal planes coinciding with the crystal faces [45,46]. BFDH theoretical crystal morphologies are calculated from the unit cell. Figures 3, 4 and 5 show the predicted BFDH crystal morphologies for forms I, III and IV of carbamazepine, respectively. They were created using the Mercury Software and packed with molecules in the corresponding lattice orientation. CBZ form I is triclinic and shows a needle habit; form III is monoclinic and has a prismatic habit; and form IV is monoclinic and has block-like habit. [47,48]

Table 1 – Comparison of Forms I, III and IV of Carbamazepine: Single Crystal

	Form I (CBMZPN11) [47]	Form III (CBMZPN22) [48,49]	Form IV (CBMZPN12) [47,50]
Empirical Formula	$C_{15}H_{12}N_2O$	$C_{15}H_{12}N_2O$	$C_{15}H_{12}N_2O$
Crystal System	Triclinic	P-Monoclinic	C-monoclinic
Space Group	P-1; P1	$P2_1/n$	C2/c
Unit Cell Dimensions: α β γ $\quad$ a b c	84.124(4)º 88.008(4)º 85.187(4)º $\quad$ 5.1705 Å 20.574(2) Å 22.245(2) Å	90º 92.953(2)º 90º $\quad$ 7.4893 Å 11.0323(5) Å 13.76.40(6) Å	90º 109.702(9)º 90º $\quad$ 26.609(4) Å 6.9269 (10) Å 13.957(2) Å
Z (Formula Unit)	Z'= 4; Z'= 8	Z= 4	Z=8 Z'=1
Density (g/cm^3)	1.31	1.38	1.27
Habit	Needle	Prism	Block

Figure 3- Form I (CBMZPN11)

Figure 4 - Form III (CBMZPN22)

Figure 5 - Form IV (CBMZPN12)

This data display which functional groups would be predominant on the different crystal faces, for each form. For carbamazepine form I, it is predicted that the crystal faces are mostly hydrophobic, showing aromatic rings on the outside (represented in grey). It is suggested that in form I the functional groups capable of forming hydrogen bond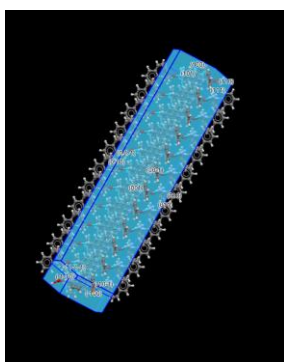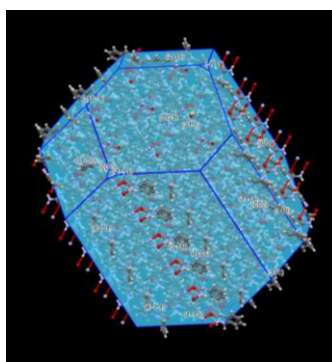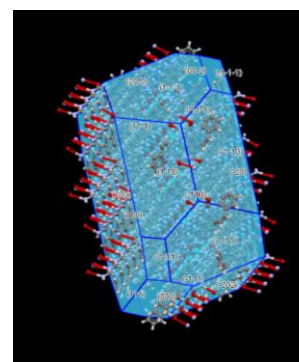s with the polymer are on the inside, interacting with other carbamazepine molecules. The opposite is showed in forms III and IV, where functional groups capable of forming hydrogen bonds with PLGA (represented in red) are on the crystal faces.

3.2. DSC Analysis

Carbamazepine, PLGA and mixtures of both were analyzed by DSC in order to understand their thermal behaviour and possible crystallinity changes[32]. Firstly carbamazepine was added to PLGA grade 75-115kDa in eight different ratios: 9.0%, 11.0%, 12.5%, 15.0%, 20.0%, 25.7%, 30.0% and 50.0% (w/w). Then, it was added in 11, 20 and 30% (w/w) to PLGA grade 90kDa, and finally in 11, 20 and 30% (w/w) to PLGA grade 154kDa. All mixtures' thermal graphs were compared to both carbamazepine and PLGA's graphs. Moreover, different loaded mixtures were compared between themselves in order to try and find if there is an effect of the drug to polymer ratio.

DSC curves recorded at 10ºC/min and obtained using three successive cycles (heating-cooling-heating). Results for first heating cycle are presented in Figures S1-S4 while cooling and second heating cycles are presented in Figures 6-9 and Tables 2-5.

Figures S1A and 6A shows results for Carbamazepine; during heating, the sample melts, which corresponds to the endothermic peak at 175.4ºC, corresponding to the melting of polymorph form III, which immediately recrystallizes as form I, represented by an exothermic peak at 176.63ºC. Following, a sharp endothermic peak is observed at 191.6ºC (T_{onset}= 190.6ºC), corresponding to the melting of form I. During the cooling stage, an exothermic peak at 152.5ºC was reported, and this was most likely due to recrystallization of carbamazepine. During the third cycle (the second heating step), only a sharp endothermic peak at 191.4ºC could be observed, that coincided with the peak observed in the first cycle, which suggest that form I recrystallized on cooling. These results are in accordance with results obtained from Krstić *et al.* and Pinto *et al.*[16,51].

The enthalpy changes measured for thermal events observed during the heating-cooling-heating cycles are summarized in Table 2. Due to the fact that carbamazepine form III melting was followed by form I recrystallization, resolution of these two overlapping events was not possible using DSC. So, it was not possible to measure the enthalpy changes of these events[51].

In summary, it could be concluded that the sample used was carbamazepine form III. In order to confirm the phase transitions observed by DSC, X-ray diffraction analysis of solid carbamazepine at 100ºC and 195ºC could be performed[51].

For PLGA, three different grades were analyzed by DSC: 75-115 kDa, 90 kDa and 154 kDa (Figure 6; Table 2). All heating-cooling-heating graphs showed similar thermal events. At around 48-55°C a glass transition step on heating cycles can be observed, characteristic of amorphous materials. Upon heating, PLGA goes from a glassy state to a rubbery state, and once cooled the opposite occurs. The temperature at which glass transition occurs is different for all three grades and it is showed in Table 2. This was in agreement with previous findings[52–54].

Table 2 - DSC Thermal Events of Carbamazepine III and PLGA (Grades 75-115; 90; and 154kDa)

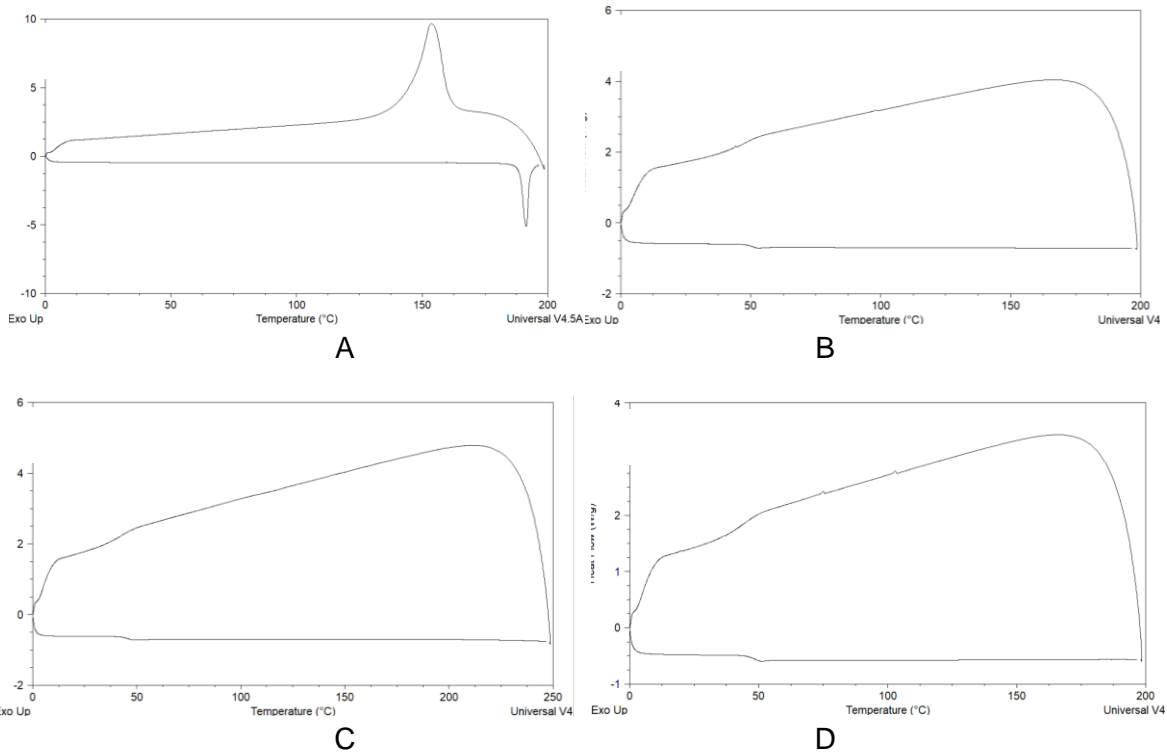| Sample		Heating cycle 1			Heating cycle 2	
		Glass Transition	Melting/ Recrystallization (Endo Peak/ Exo Peak)	Melting (On Set/ Peak, Enthalpy)	Glass Transition	(On Set/ Peak, Enthalpy)
Graph 1	Carbamazepine		175.4°C/ 176.6°C	190.6/191.6°C 96.16J/g		189.0°C/191.4°C 93.21J/g
Graph 2	PLGA 75-115kDa	55.4°C			50.6°C	
Graph 3	PLGA 90kDa	48.4°C			46.2°C	
Graph 4	PLGA 154kDa	51.5°C			48.7°C	

Figure 6 - DSC thermographs (cycles 2 and 3 only) of A): Carbamazepine, B): PLGA 75-115kDa, C): PLGA 90kDa and D): PLGA 154kDa.

For the first physical mixtures, PLGA grade 75-115kDa was used to analyze different loadings of carbamazepine by DSC. PLGA and carbamazepine were put together in aluminum pans in eight different ratios: 9.0%, 11.0%, 12.5%, 15.0%, 20.0%, 25.7%, 30.0% and 50.0% (w/w) of carbamazepine in a total weight of approximately 5mg. Results for first heating cycle are presented in Figure S2 and those for cooling and second heating cycles are presented in Figure 7. The analysis is summarised in Table 3.

These ratios were chosen based on literature. Divergences were observed when we looked for ratios used before on both spraydrying and electrospinning studies with either carbamazepine or PLGA. Baranauskaite *et al.* studied electrospun fibers formation with carbamazepine and Eudragit® E100 in 8, 16, 24, 32 and 40 wt. % of polymer[55]; while Duarte *et al.* and Warnken *et al.* used 20, 40 and 60% of carbamazepine in both HPMCAS and Eudragit® L100[18,56]. Moreover, some studies have described usage of PLGA to fabricate particles by spray drying or fibers by electrospinning. Lee *et al.* describes electrospinning using budesonide and PLGA (0.2, 0.5, 3.0 and 5.0 wt.% of polymer) [57]; Pathak *et al.* experimented with tacrolimus in drug:polymer ratios of 10:90, 15:85 and 20:80[58]; Jahangiri *et al.* experimented with 10, 15, 20% (w/v) of triamcinolone acetonide in PLGA[53]; Prabhakaran *et al.* used metronidazole in 1:20 ratio[33]. So, there was a great variety of loadings used in various papers, without any consent loading interval amongst all studies. Because of that, the strategy in the present study was to initiate experiments with a rather small quantity of drug (9%) and to keep increasing it, observing consequent alterations in DSC graphs.

Table 3- DSC Thermal Events of Mixtures of Carbamazepine and PLGA Grade 75-115kDa

Graph	CBZ (%)	PLGA 75-115 kDa (%)	Heating cycle 1			Heating cycle 2	
			Glass Transition	Melting/ Recrystallization (Endo Peak/ Exo Peak)	Melting (On Set/ Peak, Enthalpy)	Glass Transition	Melting (On Set/ Peak, Enthalpy)
Graph 5	9.0	91.0	54.5ºC	175.2ºC/ n.o.*	189.7/190.4 ºC 0.43J/g	50.8ºC	189.5/190.1ºC 0.03J/g
Graph 6	11.0	89.0	54.8ºC	175.3ºC/ 176.2ºC	189.3/191.6ºC 5.12J/g	50.0ºC	188.7/190.3ºC 1.12J/g
Graph 7	12.5	87.5	54.4ºC	175.4ºC/ 176.3ºC	189.4/190.7ºC 4.25J/g	50.1ºC	188.9/190.3ºC 0.46J/g
Graph 8	15.0	75.0	54.9ºC	175.6ºC/ n.o.*	189.6/ 190.7ºC 13.59J/g	50.1ºC	189.1/190.4ºC 3.81J/g
Graph 9	20.0	80.0	55.1ºC	175.2ºC/ 176.3ºC	189.3/191.5ºC 15.98J/g	50.6ºC	187.2/190.4ºC 10.09J/g
Graph 10	25.7	74.3	55.3ºC	175.2ºC/ 176.4ºC	189.6/190.7ºC 14.25J/g	50.8ºC	188.0/190.7ºC 5.34J/g
Graph 11	30.0	70.0	56.2ºC	175.3ºC/ 176.4ºC	189.5/191.5ºC 17.02J/g	50.5ºC	187.8/190.4ºC 9.37J/g
Graph 12	50.0	50.0	55.8ºC	174.7ºC/ 176.5ºC	189.9/ 191.2ºC 38.44J/g	50.0ºC	188.6/190.4ºC 30.04J/g

*not observed

Exo up

A

B

C

D

E

F

G

H

Figure 7- DSC thermographs (cycles 2 and 3) of A): 9% Carbamazepine in PLGA 75-115kDa, B): 11% Carbamazepine in PLGA 75-115kDa, C): 12.5% Carbamazepine in PLGA 75-115kDa D): 15% Carbamazepine in PLGA 75-115kDa, E): 20% Carbamazepine in PLGA 75-115kDa, F): 25.7%

Then, carbamazepine was added to PLGA grade 90kDa in aluminum pans, in total of approximately 5mg. The loadings tested were 11.0%, 20.0%, and 30.0% (w/w) of carbamazepine. Results for first heating cycle are presented in Figure S3 and those for cooling and second heating cycles are presented in Figure 8. The analysis is summarised in Table 4.

Table 4- DSC Thermal Events of Mixtures of Carbamazepine and PLGA Grade 90kDa

Graph	CBZ (%)	PLGA 90 kDa (%)	Heating cycle 1			Heating cycle 2	
			Glass Transition	Melting/ Recrystallization (Endo Peak/ Exo Peak)	Melting (On Set/ Peak, Enthalpy)	Glass Transition	Melting (On Set/ Peak, Enthalpy)
Graph 13	11.0	89.0	48.6ºC	174.1ºC/ 175.7ºC	187.7/189.9º C 4.57 J/g	48.7ºC	182.8/188.3ºC 1.27 J/g
Graph 14	20.0	80.0	41.4ºC	n.o.*	n.o.*	41.8ºC	n.o.*
Graph 15	30.0	70.0	48.7ºC	174.6ºC/ 175.9ºC	187.9/190.2º C 17.92 J/g	47.9ºC	188.9/190.7ºC 25.24 J/g

*not observed

Exo up

A   B

C

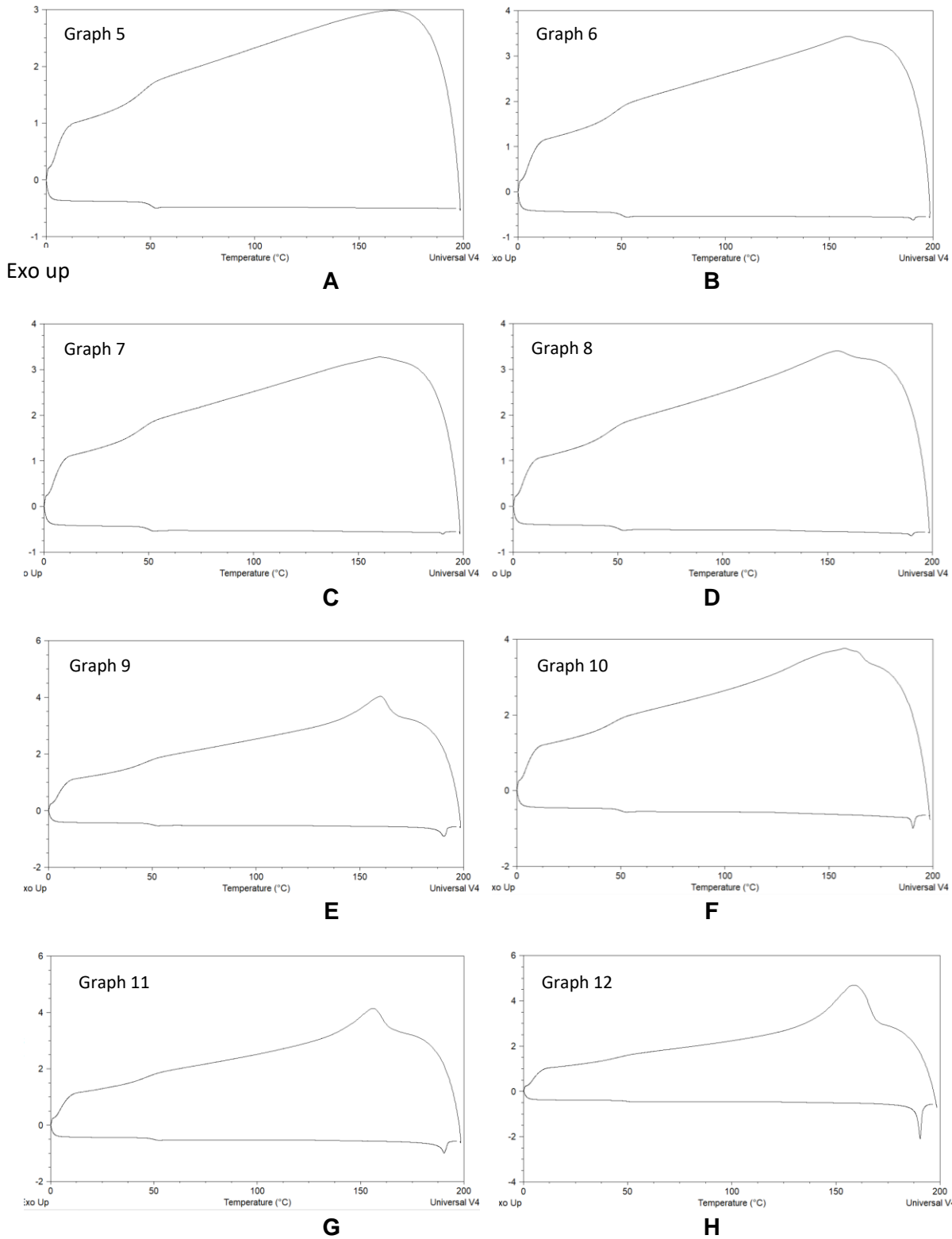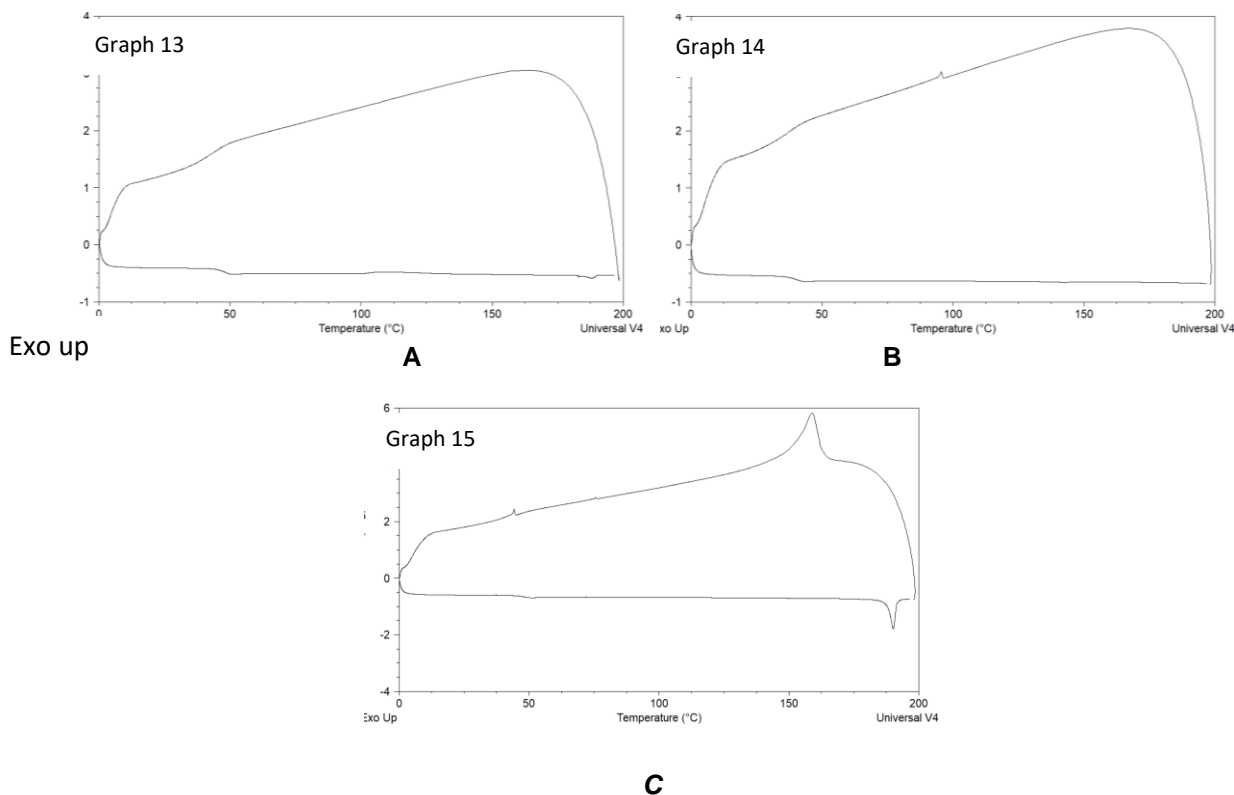*Figure 8 - DSC thermographs (cycles 2 and 3) of A): 11% Carbamazepine in PLGA 90kDa, B): 20% Carbamazepine in PLGA 90kDa, C): 30% Carbamazepine in PLGA 90KDa.*

Finally, carbamazepine was added to PLGA grade 154kDa together in aluminum pans, in total of approximately 5mg. The loadings tested were the same as previous: 11.0%, 20.0%, and 30.0% (w/w) of carbamazepine. Results for first heating cycle are presented in Figure S3 and those for cooling and second heating cycles are presented in Figure 8. The analysis is summarised in Table 5.

Table 5- DSC Thermal Events of Mixtures of Carbamazepine and PLGA Grade 154kDa.

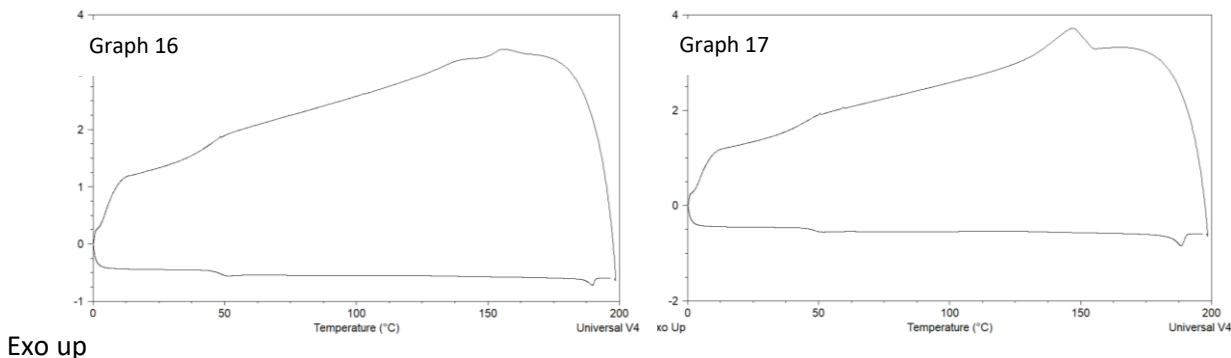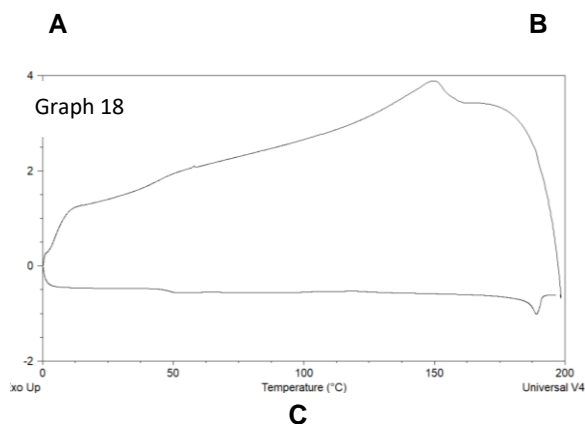| Graph | CBZ (%) | PLGA 154 kDa (%) | Heating cycle 1 | | | Heating cycle 2 | |
			Glass Transition	Melting/ Recrystallization (Endo Peak/ Exo Peak)	Melting (On Set/ Peak, Enthalpy)	Glass Transition	Melting (On Set/ Peak, Enthalpy)
Graph 16	11.0	89.0	55.5ºC	173.9ºC/ 174.5ºC	188.1/190.3ºC 7.58J/g	48.8ºC	186.7/189.7ºC 2.49J/g
Graph 17	20.0	80.0	50.3ºC	173.8ºC/ 175.1ºC	188.0/ 189.9ºC 14.70J/g	48.4ºC	183.7/ 188.3ºC 16.22J/g
Graph 18	30.0	70.0	57.5ºC	174.4ºC/ 175.4ºC	186.3/190.7ºC 24.54J/g	48.5ºC	185.0/ 189.1ºC 15.83J/g

Exo up

A   B

C

Figure 9 - DSC thermographs (cycles 2 and 3) of A): 11% Carbamazepine in PLGA 154kDa, B): 20% Carbamazepine in PLGA 154kDa, C): 30% Carbamazepine in PLGA 154KDa.

DSC thermograms demonstrate how heat flow varies as a function of temperature for PLGA, carbamazepine, and carbamazepine-PLGA mixtures. For PLGA grade 75-115kDa mixtures (Figure 7A-H), it can be observed that all loadings of carbamazepine led to similar graphs. In these graphs, PLGA's corresponding glass transition is shown, as well as the corresponding melting and crystallization of carbamazepine form III and the melting of form I. The variation of glass transition temperatures among the graphs is insignificant. It is also similar to PLGA (Figure 6B): the mean value of eight mixtures is approximately 1.8 and 2.0% lower that pure PLGA for cycles 1 and 3, respectively.

No solvent was used, as drug and polymer were mixed during the first cycle, while both the drug and polymer were forced to undergo melting and transition to plastic phase, respectively. If they were to interact and form a new solid dispersion, the new phase would show a new glass transition temperature (Tg), higher or lower than plain PLGA's. This new phase could either behave as a stable or unstable phase, and DSC analysis would be helpful to evaluate this. DSC graphs would also be useful for optimization of the maximum drug loading quantity for PLGA, in which the newly formed phase would remain stable. Hence, if carbamazepine and PLGA would form a new phase, we would find modifications of thermal events on DSC, and a different Tg, which did not happen.

Therefore, we can hypothesize that the presence of carbamazepine does not affect the Tg of the polymer, in any of the drug loadings tested. So, it is most likely that the polymer and drug do not interact and, instead, they behave independently.

The same hypothesis seems applicable when interpreting the melting enthalpy of Figure 7A-H. The mixtures melting events have been slightly shifted to between 189.5ºC and 191.7ºC, which corresponds to the melting of carbamazepine form I. When we evaluated melting enthalpies of these samples, a direct relationship between enthalpy and concentration of carbamazepine was established (Figure 10). This goes according to the supposition that carbamazepine and PLGA behave separately and that the presence of PLGA does not influence carbamazepine's thermal behaviour. In both heating cycles (cycles 1 and 3), the higher the percentage of carbamazepine, the higher the melting enthalpy.
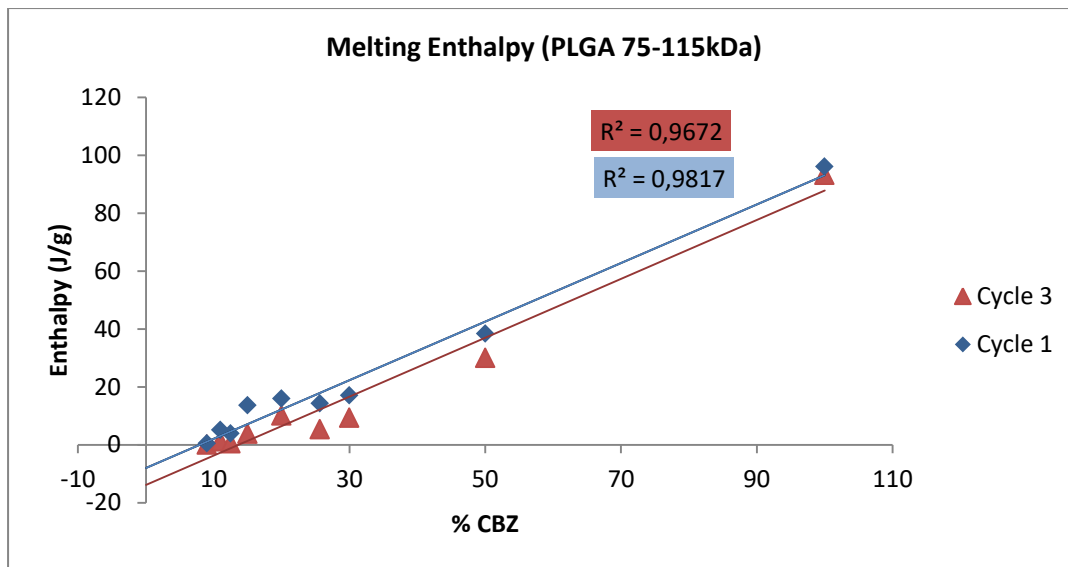
Figure 10 - Plot of Melting Enthalpy of CBZ as a function of CBZ concentration (cycles 1 and 3) – PLGA 75-115kDa physical mixtures

After this, melting enthalpy of carbamazepine- PLGA 90kDA mixtures was also analyzed in 11%, 20% and 30% (data shown in figure S5) but these were not conclusive. On one hand, for 11% and 30% the glass transition temperatures were 48.7ºC±0.07 and 48.4ºC±0.5 for cycles 1 and 3, respectively. On the other hand, for 20% carbamazepine, Tg was observed at 41.4ºC and 41.8ºC. Comparing to PLGA's Tg (48.4 for cycle 1 and 46.2 for cycle 3), the 20% sample's results show a deviation of about 10% and 14% on cycle 1 and 3, respectively.

There is no apparent justification to this deviation. It could be a procedure mistake or it could mean that for 20% loading of carbamazepine on PLGA grade 90kDa the glass transition temperature is, in fact, lower; and that this concentration of carbamazepine the polymer and drug form a new amorphous phase. Moreover, no other thermal event is observed in this graph, not even melting, which suggests that the sample is not crystalline. DSC is able to detect crystallinity only where at least 2% of the material is crystalline[22]. However, this is unlike what happens with the two other grades of PLGA tested; and it does not happen in either 11% or 30% samples. Further investigation should be made to verify this value.

Carbamazepine plus PLGA 154kDa mixtures were also analyzed in 11%, 20% and 30%. The results were similar to those observed with PLGA 75-115kDa. Tg values were similar between samples and melting enthalpies were directly related to percentage of carbamazepine in sample (Figure 11), as observed for PLGA 75-115kDa. Furthermore, the direct relationship found between the melting enthalpy and the percentage of carbamazepine allows the calculation of the quantity of carbamazepine in any mixture through the line equation. It is possible to use DSC instead of other methods, such as HPLC, to obtain the quantity of drug in a sample.
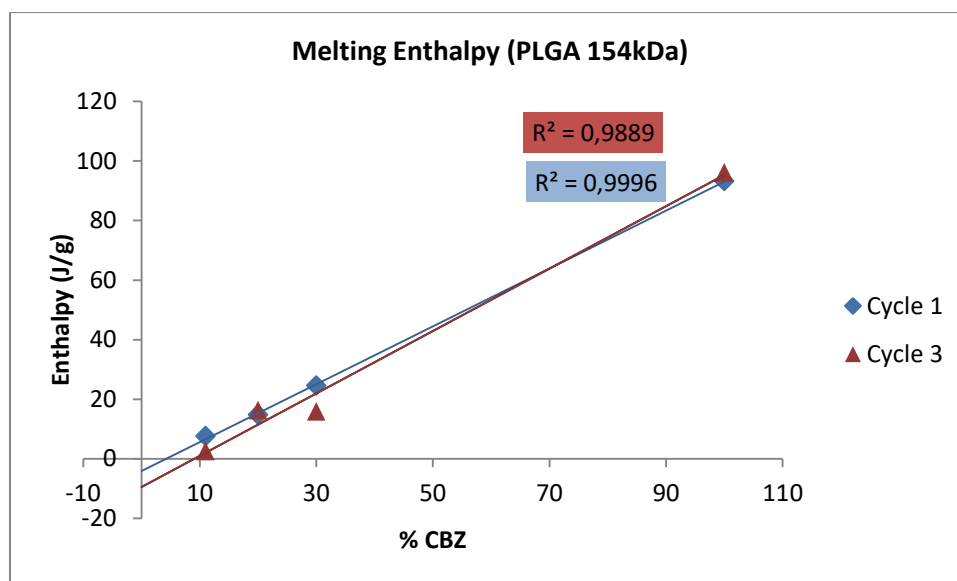
Figure 11 - Plot of Melting Enthalpy of CBZ as a function of CBZ concentration (cycles 1 and 3) – PLGA 154kDa physical mixtures

Based on the results so far, carbamazepine and PLGA do not appear to interact and behave as one amorphous new phase. This goes accordingly to the fact that carbamazepine has a higher tendency to being in a crystalline form, rather than in an amorphous one. And also to the fact that carbamazepine form I does not show many functional groups free to interact through hydrogen bonds with PLGA. Instead, the crystals are organized in a needle habit, in which the aromatic rings face the outside, and hydrogen bonds are formed between carbamazepine molecules within the crystals.

In this study drug and polymer were not dissolved in any solvent, instead, the mixture underwent high temperatures in the DSC furnace. When heated together, drug and polymer molecules do not appear to interact with one another, which is accordingly to what crystalline predictions of CBZ form I suggest. Carbamazepine seems to crystallize as form I upon cooling the melt, which has higher tendency to form hydrogen bonds between its own molecules leaving none of the functional groups available to interact with the polymer. The high hydrogen bond propensity in between molecules of CBZ has been previously reported[43].

Perhaps, a mixture of carbamazepine and PLGA in a solvent at room temperature, they could interact differently due to evidence showing that carbamazepine would be in form III. Form III, unlike form I, could be able to form hydrogen bonds with PLGA due to having its aromatic rings facing the inside and, in contrast, its functional groups capable of forming hydrogen bonds with PLGA on the crystal faces. This hypothesis should be verified in future experiments.

All these results indicate that PLGA and carbamazepine most probably do not chemically or physically interact. Initially, drug-polymer interaction and formation of an amorphous solid dispersion seemed ideal in this study, due to carbamazepine's solubility increase. However, this can be a positive consequence. Amorphous substances are often much less stable[59] while

crystalline tend to be stable for longer periods of time. Moreover, there is a parameter other than amorphization/polymorphism that can be adjusted to maximize drug's rate of dissolution: the surface area. Moreover, Duarte *et al.* revealed that for carbamazepine, the reduction of particle size is more important than its amorphous status[18]. And perhaps, by having a nanoscale crystalline drug, the stability could be superior than if it were amorphous. Future stability studies should be performed in order to complement this hypothesis.

3.3.   Morphology and Solvent

Morphological aspects and drug-loading efficiency of the obtained fibers or particles rely greatly on the technological parameters used during the production[52] as well as the formulation itself[28,40,52]. Multiple solvents, such as acetone, tetrahydrofuran, dichloromethane (DCM), acetonitrile, dimethylformamide (DMF), and chloroform, have been described in literature as capable to form good PLGA electrospinning and/or electrospraying solutions[40,57].

Two solvent mixtures - acetone, and DCM:DMF (50:50) - were tested to dissolve four PLGA grades (17kDa, 75-115KDa, 90KDa and 154kDa), in various percentages. The resulting electrospun fibers were characterized with respect to the morphology under scanning electron microscopy (SEM). The most promising fibers were obtained with 154kDa PLGA dissolved in acetone (20% m/v).

PLGA fibers were produced successfully using the selected parameters established for the electrospinning procedure. Visually uniform white fibers were observed from the equipment collector, which means that the viscosity of the polymer solution is above a threshold, so that the ejected solution does not break down as microdroplets[2]. The obtained fibers resulted from a solution of 20% PLGA 154kDa in acetone, spun by a syringe pump at flow rate of 0.6 mL/hr into a non-woven form nanofibrous membrane onto a collection plate at room temperature. The voltage was set to 10 kV, while the travel distance from the needle to the collection plate was 20 cm.

The parameters as well as the PLGA grade and solvent were optimized by SEM. Four different PLGA grades (17, 90, 75-115 and 154 kDa) and two different mixtures of solvents (acetone; and DCM+DMF) were electrospun and later characterized by SEM. Images of the 17kDa PLGA (data not shown) dissolved in both solvents suggest the formation of only beads; while images of electrospun 90kDa and 75-115kDa PLGA show the presence of both beads and fibers (beads-in-string[27]), though 90kDa PLGA (data not shown) appears to form more beads than the 75-115kDa PLGA (Fig. 12). Smooth fibers, with approximate size of 2.36 µm, were achieved by electrospinning from 154kDa PLGA dissolved in acetone (Fig. 13). This indicates that the increase of PLGA grade could be related to the increase of PLGA electrospinnability[40].
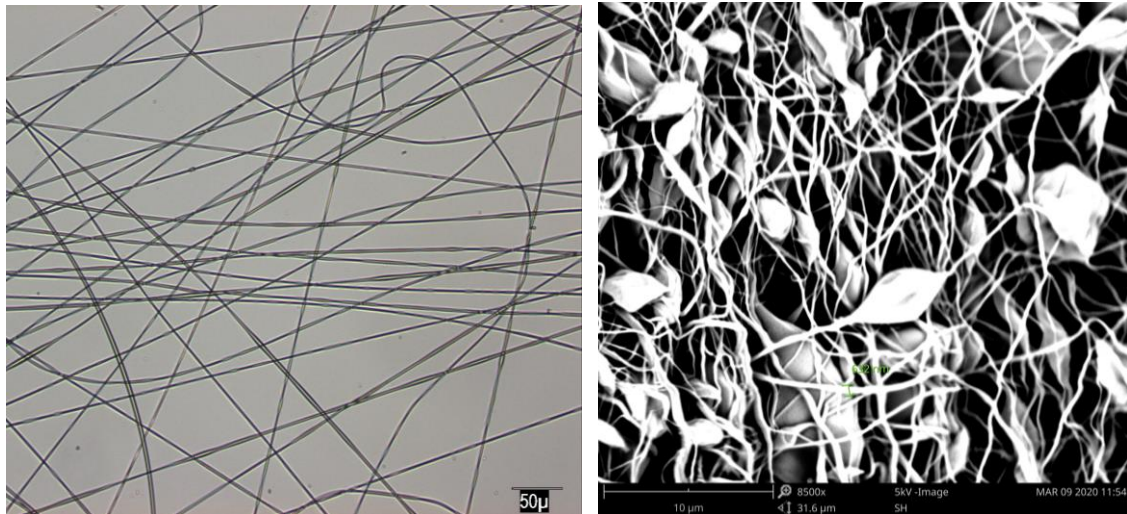
Figure 12 - Electrospun PLGA: beads-in-strings of PLGA 75-115KDa of 20% in acetone (flow rate= 0.6 ml/hr, voltage= 10 KV, distance plate= 20 cm).
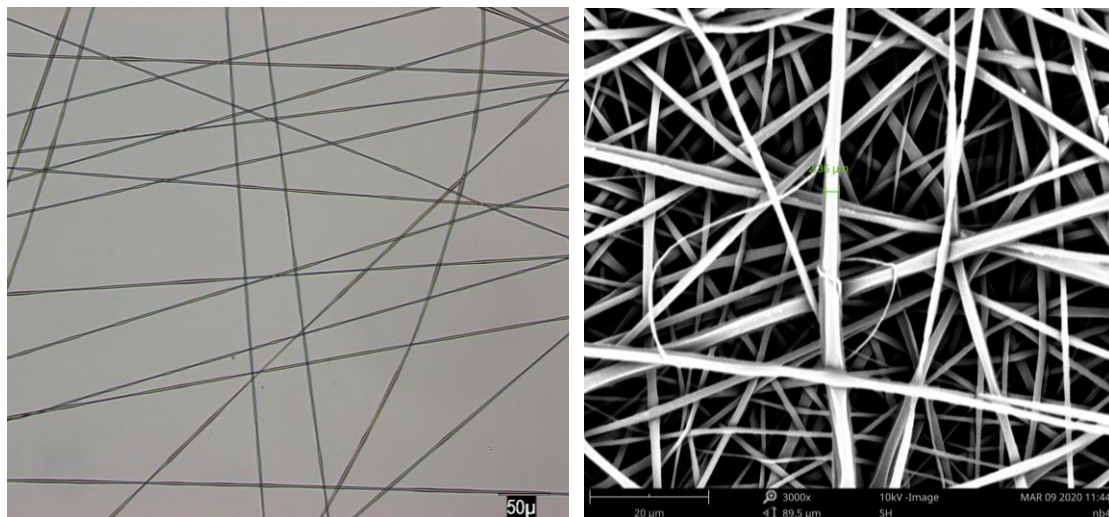
Figure 13 - Electrospun PLGA: fibers of PLGA 154KDa of 20% in acetone (flow rate= 0.6 ml/hr, voltage= 10 KV, distance plate= 20 cm).

Such results are similar to what Liu *et al.* discovered and some factors might explain it. The difference in the morphology of electrospun products may be due to different elasticity of polymer solutions. In the electrospinning process, solution rheological properties play a critical role on the formation of the fibers. The three main rheological factors are solution viscosity, surface tension, and the net charge density carried by the electrospinning jet. These aspects can influence intermolecular interactions and, therefore, chain entanglement and relaxation time[40].

The rheological properties of the high molecular weight PLGA could guarantee sufficient intermolecular interactions, needed for good fiber generation. It has been described that higher polymer molecular weight and higher polymer concentration are correlated to higher viscosity of the electrospun solution; and that higher polymer concentration is correlated to an increased surface tension.

The choice of solvent can also contribute to changes in viscosity, influencing the morphology and mechanical properties of the electrospun solution. Different solvents also differ in surface tension, intrinsic viscosity, and solvent evaporation rate. During the electrospinning process, high evaporation rate, high net charge density and low surface tension tended to favor the entanglements and, therefore, fiber formation. The viscosity of the electrospun solution must not be so low that it cannot form entanglements required for fiber formation, but also not so high that it prevents polymer motion induced by the electric field. Moreover, a higher viscosity might indicate a higher intermolecular interaction, crucial to resist the change caused by the external force[40,60–62].

3.4. Electrospun Fibers DSC Analysis

154kDa PLGA was compared with electrospun fibers of 20% 154kDa PLGA in acetone (Figure S6). Both graphs showed similar thermal events, namely a glass transition step in the first and third cycles. We observed that PLGA electrospun fibers presented a transition glass temperature of 49.75ºC in the first cycle, and 47.70ºC in the third cycle. PLGA, on the other hand, presented a Tg of 51.48ºC in the first cycle, and 48.66ºC in the third cycle. The small differences of 2.1 and 2.2% between both first and third cycles' Tg appears to be insignificant. Further work should be done, inclusively, formulation and analysis of fibers loaded with carbamazepine.

In short, pre-formulation studies indicate that drug and polymer molecules most probably do not interact. Thermal DSC graphs, along with the crystal data, suggested that CBZ and PLGA behave independently, therefore, not forming a stable amorphous phase (ASD). Even though hydrogen bonds could be expected when looking at chemical structures, crystal structure data of CBZ showed that form I, which crystallises from cooling molten CBZ, has a lot of hydrogen bonds between its molecules so it could be argued that they are preferred over interacting with the polymer.

DSC thermal analysis concludes that, for all grades of PLGA tested, no new phase with a characteristic Tg was formed. In that hypothetical case, the best loading at which the new formed phase would remain stable could be investigated through DSC. However, no ideal loading could be reported in this study. We can hypothesize that the presence of carbamazepine does not affect the Tg of the polymer, and that CBZ and PLGA behave independently. CBZ remains crystalline when in a mixture with PLGA.

Nonetheless, the lack of interaction observed could be a positive point due to higher stability of crystalline forms compared to amorphous forms. Besides, there is a parameter other than amorphization that can be adjusted to maximize drug's rate of dissolution: the surface area, which has been reported to be more important for carbamazepine than its amorphization. So, further studies should be performed to understand if by having a nanoscale crystalline drug, the stability could be superior than if it were amorphous.

In thermal graphs, a direct relationship between the percentage of carbamazepine and melting was reported, which is accordingly to the lack of interaction explained before. Such information can be useful because it allows the use of DSC, instead of other relatively slower methods, like HPLC, to calculate the quantity of drug in a given sample.

As far as fiber morphology is concerned, various PLGA grades and solvents were tested, 154kDa PLGA and acetone being the best ones. Also, a relationship between an increase of PLGA grade and an increase of PLGA's electrospinnability was found. The choice of solvent is important due to its implications on the rheological properties, such as solution viscosity, surface tension, and the net charge density carried by the electrospinning jet.

Finally, thermal analysis of fabricated fibers revealed no differences when comparing to plain PLGA analysis. However, we cannot conclude that CBZ-loaded fibers would behave similar to CBZ-PLGA mixtures as well.

4. Conclusion

This study opens up new routes for fabrication of carbamazepine-loaded nanofibers, through electrospinning. Crystal data confirm lack of interaction between the drug and the polymer because CBZ form I has higher tendency to form bonds between its own molecules and not with PLGA. In mixture, thermal behaviour of CBZ and PLGA remain independent of each other, showing that no amorphous dispersion is formed and, instead, CBZ remains crystalline. However, crystallinity could provide higher long-term stability; and reducing particle size to nanoscale could be accomplished by electrospinning, improving dissolution rate. The exact behaviour of the electrospun carbamazepine fibers requires further research.

Studies of PLGA fibers morphology showed that PLGA electrospinnability increased as its grade also increased. The choice of solvent was proven to influence the formation of fibers, due to its effects on rheological properties. The higher grade tested of PLGA, 154kDa, dissolved at 20% w/v in acetone was the only one capable of forming uniform fibers under SEM. In addition, the properties of electrospun PLGA-only fibers are similar to those of the free PLGA.

Fibers prepared by electrospinning can potentially be a good alternative to current therapies available. Electrospinning is a relatively easy method that allows fabrication of coaxial fibers that could join chemical and genetical therapeutics, in each layer of the fibers. Regarding the outer layer, further data must be accessed in order to successfully understand stability, loading capacity and drug release pattern.

5. Future Perspectives

Our data show that CBZ and PLGA do not interact when in physical mixtures, warranting further investigation about their behaviour when in electrospun fibers. Fibers loaded with carbamazepine should be fabricated – in 11, 20 and 30%, so that it is possible to compare with results of mixtures of CBZ-PLGA 154kDa. Despite observation of similar behaviour in a sample of plain PLGA and a sample of electrospun PLGA fibers, carbamazepine-in-PLGA fibers could behave differently than physical mixtures of CBZ and PLGA, already analysed by DSC. So, firstly CBZ-PLGA interaction in electrospun fibers should be studied. DSC analysis should be run on these loaded-fibers and, therefore, lack of interaction could be confirmed[63].

In our experiments, no solvent was used, as drug and polymer were mixed together during the first cycle, while both the drug and polymer were forced to undergo melting and transition to plastic phase, respectively. In order to confirm if the presence of the solvent and/or the process of electrospinning have any effect on CBZ or PLGA conduct, more experiments should be run. Although the same behaviour is expected, there are two possible scenarios: 1) DSC graphs look similar to previous ones, showing that they in fact do not interact; or 2) DSC graphs hint possible interactions between drug and polymer, with formation of a new amorphous phase.

In the future, maximum loading capacity must be determined either by DSC experiments or by HPLC. It reflects the limit quantity of carbamazepine that PLGA fibers can take.

The present study found that CBZ and PLGA do not form a new amorphous phase and, instead, CBZ remains crystalline. From a stability perspective this can be a positive outcome because crystalline substances are often more stable long-term. To understand carbamazepine-in-PLGA fiber behaviour, and its possible future applicability, stability tests must be performed. Stability studies should include the evaluation of organoleptic and morphological characteristics, carbamazepine content, and dissolution pattern, under long-term conditions (25ºC/ 60% relative humidity (RH)) and accelerated stress conditions (40ºC/ 75% RH), for 6 months[18,20,55]. Evaluation of morphology under SEM should reveal minimal physical changes during the study period. To estimate CBZ content, DSC experiments could be run in order to calculate carbamazepine quantity after 6 months; alternatively, HPLC analysis could be performed. Dissolution studies after the study time should reveal a similar profile to the initial one observed.

In vitro dissolution assays should be planned to understand the drug release pattern, and help adjust the formulation to a desired prolonged released. An *in vitro* model that simulates brain environment should be used.

If CBZ-PLGA's lack of interaction does not enhance stability, another drug and/or PLGA should be tried. The choice of a new drug should be made based on abundance of functional groups suitable for hydrogen bonding (chemical and crystal analysis). Based on the chemical structure alone, phenytoin could be a good option, considering it has two HDB and four HBA. Plus, it is a widely used broad spectrum antiepileptic drug, often comparable to CBZ[64]. Instead, trying a different polymer could be a good alternative. In that case, a polymer with higher Tg, for instance HPMCAS, should be used of because high Tg have been proved to enhance anti-plasticization and lowering the molecular mobility of the drug, thereby being better ASD co-formers[20,22].

The potential of coaxial electrospinning in formation of core-shell fibers can be utilised in delivery combinations of drugs and genetic therapy, with the additional advantage of controlling release profiles. Further investigation must go on to fulfil the goal of creating coaxial nanofiber for surgical implantation in epilepsy patients.

Bibliography

1. Costa, D., Valente, A. J. M., Miguel, M. G. & Queiroz, J. Plasmid DNA hydrogels for biomedical applications. *Adv. Colloid Interface Sci.* **205**, 257–264 (2014).

2. van Tienderen, G. S. *et al.* Advanced fabrication approaches to controlled delivery systems for epilepsy treatment. *Expert Opin. Drug Deliv.* **15**, 915–925 (2018).

3. Thijs, R. D., Surges, R., O'Brien, T. J. & Sander, J. W. Epilepsy in adults. *Lancet* **393**, 689–701 (2019).

4. Manford, M. Recent advances in epilepsy. *J. Neurol.* **264**, 1811–1824 (2017).

5. Fisher, R. S. *et al.* ILAE Official Report: A practical clinical definition of epilepsy. *Epilepsia* **55**, 475–482 (2014).

6. Sun, J. J., Xie, L. & Liu, X. D. Transport of carbamazepine and drug interactions at blood-brain barrier. *Acta Pharmacol. Sin.* **27**, 249–253 (2006).

7. West, S., Nolan, S. J. & Newton, R. Surgery for epilepsy: A systematic review of current evidence. *Epileptic Disord.* **18**, 113–121 (2016).

8. Kwan, P. & Sperling, M. R. Refractory seizures: Try additional antiepileptic drugs (after two have failed) or go directly to early surgery evaluation? *Epilepsia* **50**, 57–62 (2009).

9. Proctor, C. M. *et al.* Electrophoretic drug delivery for seizure control. *Sci. Adv.* **4**, 1–8 (2018).

10. Fisher, R. S. & Ho, J. Potential new methods for antiepileptic drug delivery. *CNS Drugs* **16**, 579–593 (2002).

11. Fricke-Galindo, I., LLerena, A., Jung-Cook, H. & López-López, M. Carbamazepine adverse drug reactions. *Expert Rev. Clin. Pharmacol.* **11**, 705–718 (2018).

12. Abou-Khalil, B. W. Antiepileptic drugs. *Contin. Lifelong Learn. Neurol.* **22**, 132–156 (2016).

13. Nieber, K. Carbamazepine. *Dtsch. Medizinische Wochenschrift* **129**, 627–629 (2004).

14. Wenju, L., Leping, D., Black, S. & Hongyuan, W. Solubility of carbamazepin (form III) in different solvents from (275 to 343) K. *J. Chem. Eng. Data* **53**, 2204–2206 (2008).

15. Collaborators, N. A. S. C. E. T. A Comparison of Valproate With Carbamazepine for the Treatment of Complex Partial Seizures and Secondarily Generalized Tonic-Clonic Seizures in Adults. The Department of Veterans Affairs Epilepsy Cooperative Study No. 264 Group. *N. Engl. J. Med.* **329**, 977–986 (1991).

16. Krstić, M., Popović, M., Dobričić, V. & Ibrić, S. Influence of solid drug delivery system formulation on poorly water-soluble drug dissolution and permeability. *Molecules* **20**, 14684–14698 (2015).

17. Potschka, H., Fedrowitz, M. & Löscher, W. Brain Access and Anticonvulsant Efficacy of Carbamazepine, Lamotrigine, and Felbamate in ABCC2/MRP2-Deficient TR- Rats.

Epilepsia **44**, 1479–1486 (2003).

18.   Duarte, Í. *et al.* Production of nano-solid dispersions using a novel solvent-controlled precipitation process — Benchmarking their in vivo performance with an amorphous micro-sized solid dispersion produced by spray drying. *Eur. J. Pharm. Sci.* **93**, 203–214 (2016).

19.   Könczöl, Á. & Dargó, G. Brief overview of solubility methods: Recent trends in equilibrium solubility measurement and predictive models. *Drug Discov. Today Technol.* **27**, 3–10 (2018).

20.   Ziaee, A. *et al.* Amorphous solid dispersion of ibuprofen: A comparative study on the effect of solution based techniques. *Int. J. Pharm.* **572**, 118816 (2019).

21.   Leleux, J. & Williams, R. O. Recent advancements in mechanical reduction methods: Particulate systems. *Drug Dev. Ind. Pharm.* **40**, 289–300 (2014).

22.   Yu, D. G., Li, J. J., Williams, G. R. & Zhao, M. Electrospun amorphous solid dispersions of poorly water-soluble drugs: A review. *J. Control. Release* **292**, 91–110 (2018).

23.   Baghel, S., Cathcart, H. & O'Reilly, N. J. Polymeric Amorphous Solid Dispersions: A Review of Amorphization, Crystallition, Stabilization, Solid-State Characterization, and Aqueous Solubilization of Biopharmaceutical Classification System Class II Drugs. *J. Pharm. Sci.* **105**, 2527–2544 (2016).

24.   Bhardwaj, N. & Kundu, S. C. Electrospinning: A fascinating fiber fabrication technique. *Biotechnol. Adv.* **28**, 325–347 (2010).

25.   Vass, P. *et al.* Scaled-Up production and tableting of grindable electrospun fibers containing a protein-type drug. *Pharmaceutics* **11**, 1–12 (2019).

26.   Zupančič, Š. Core-shell nanofibers as drug delivery systems. *Acta Pharm.* **69**, 131–153 (2019).

27.   Qi, H., Hu, P., Xu, J. & Wang, A. Encapsulation of drug reservoirs in fibers by emulsion electrospinning: Morphology characterization and preliminary release assessment. *Biomacromolecules* **7**, 2327–2330 (2006).

28.   Pawar, A., Thakkar, S. & Misra, M. A bird's eye view of nanoparticles prepared by electrospraying: advancements in drug delivery field. *J. Control. Release* **286**, 179–200 (2018).

29.   Vass, P. *et al.* Scale-up of electrospinning technology: Applications in the pharmaceutical industry. *Wiley Interdiscip. Rev. Nanomedicine Nanobiotechnology* 1–24 (2019). doi:10.1002/wnan.1611

30.   Zhu, W., Masood, F., O'Brien, J. & Zhang, L. G. Highly aligned nanocomposite scaffolds by electrospinning and electrospraying for neural tissue regeneration. *Nanomedicine Nanotechnology, Biol. Med.* **11**, 693–704 (2015).

31.   Saraf, A., Baggett, L. S., Raphael, R. M., Kasper, F. K. & Mikos, A. G. Regulated non-viral gene delivery from coaxial electrospun fiber mesh scaffolds. *J. Control. Release* **143**, 95–103 (2010).

32.	Ali, I. H., Khalil, I. A. & El-Sherbiny, I. M. *Single-Dose Electrospun Nanoparticles-in-Nanofibers Wound Dressings with Enhanced Epithelialization, Collagen Deposition, and Granulation Properties. ACS Applied Materials and Interfaces* **8**, (2016).

33.	Prabhakaran, M. P., Zamani, M., Felice, B. & Ramakrishna, S. Electrospraying technique for the fabrication of metronidazole contained PLGA particles and their release profile. *Mater. Sci. Eng. C* **56**, 66–73 (2015).

34.	Jezela-Stanek, A. & Chorostowska-Wynimko, J. Beyond the lungs: Alpha-1 antitrypsin's potential role in human gestation. *Adv. Clin. Exp. Med.* **28**, 0–0 (2019).

35.	Prabu, G. T. V & Dhurai, B. A Novel Profiled Multi-Pin Electrospinning System for Nanofiber Production and Encapsulation of Nanoparticles into Nanofibers. *Nature* 1–11 (2020). doi:10.1038/s41598-020-60752-6

36.	Zhao, X. H., Tay, F. R., Fang, Y. J., Meng, L. Y. & Bian, Z. Topical application of phenytoin or nifedipine-loaded PLGA microspheres promotes periodontal regeneration in vivo. *Arch. Oral Biol.* **97**, 42–51 (2019).

37.	Gentile, P., Chiono, V., Carmagnola, I. & Hatton, P. V. An overview of poly(lactic-co-glycolic) Acid (PLGA)-based biomaterials for bone tissue engineering. *Int. J. Mol. Sci.* **15**, 3640–3659 (2014).

38.	Hirenkumar, M. & Steven, S. Poly Lactic-co-Glycolic Acid (PLGA) as Biodegradable Controlled Drug Delivery Carrier. *Polymers (Basel).* **3**, 1–19 (2012).

39.	Buanz, A. B. M. *et al.* Ink-jet printing versus solvent casting to prepare oral films: Effect on mechanical properties and physical stability. *Int. J. Pharm.* **494**, 611–618 (2015).

40.	Liu, X. *et al.* Electrospinnability of Poly Lactic-co-glycolic Acid (PLGA): the Role of Solvent Type and Solvent Composition. *Pharm. Res.* **34**, 738–749 (2017).

41.	MacRae, C. F. *et al.* Mercury 4.0: From visualization to analysis, design and prediction. *J. Appl. Crystallogr.* **53**, 226–235 (2020).

42.	Groom, C. R., Bruno, I. J., Lightfoot, M. P. & Ward, S. C. The Cambridge structural database. *Acta Crystallogr. Sect. B Struct. Sci. Cryst. Eng. Mater.* **72**, 171–179 (2016).

43.	Verma, V., Zeglinski, J., Hudson, S., Davern, P. & Hodnett, B. K. Dependence of Heterogeneous Nucleation on Hydrogen Bonding Lifetime and Complementarity. *Cryst. Growth Des.* **18**, 7158–7172 (2018).

44.	Shmool, T. A., Hooper, P. J., Schierle, G. S. K., derWalle, C. F. va. & Zeitler, J. A. Terahertz spectroscopy: An investigation of the structural dynamics of freeze-dried poly lactic-co-glycolic acid microspheres. *Pharmaceutics* **11**, (2019).

45.	Mahé, N. *et al.* Solid-state properties and dehydration behavior of the active pharmaceutical ingredient potassium guaiacol-4-sulfonate. *Cryst. Growth Des.* **13**, 3028–3035 (2013).

46.	Donnay, J.D.H.; Harker, D. *Am. Mineral, 22.* (1937).

47.	Grzesiak, A. L., Lang, M., Kim, K. & Matzger, A. J. Comparison of the Four Anhydrous Polymorphs of Carbamazepine and the Crystal Structure of Form I. *J. Pharm. Sci.* **92**,

2260–2271 (2003).

48. Kogan, A. *et al.* Crystallization of carbamazepine pseudopolymorphs from nonionic microemulsions. *Langmuir* **24**, 722–733 (2008).

49. Sovago, I. *et al.* Electron density, disorder and polymorphism: High-resolution diffraction studies of the highly polymorphic neuralgic drug carbamazepine. *Acta Crystallogr. Sect. B Struct. Sci. Cryst. Eng. Mater.* **72**, 39–50 (2016).

50. Lang, M., Kampf, J. W. & Matzger, A. J. Form IV of carbamazepine. *J. Pharm. Sci.* **91**, 1186–1190 (2002).

51. Pinto, M. A. L., Ambrozini, B., Ferreira, A. P. G. & Cavalheiro, É. T. G. Thermoanalytical studies of carbamazepine: Hydration/dehydration, thermal decomposition, and solid phase transitions. *Brazilian J. Pharm. Sci.* **50**, 877–884 (2014).

52. De Oliveira, A. R. *et al.* Structural and thermal properties of spray-dried methotrexate-loaded biodegradable microparticles. *J. Therm. Anal. Calorim.* **112**, 555–565 (2013).

53. Jahangiri, A. *et al.* Application of electrospraying as a one-step method for the fabrication of triamcinolone acetonide-PLGA nanofibers and nanobeads. *Colloids Surfaces B Biointerfaces* **123**, 219–224 (2014).

54. Barbosa, J. *et al.* Development and Characterization of an Intraocular Biodegradable Polymer System Containing Cyclosporine-A for the Treatment of Posterior Uveitis 2 . Experimental Procedure 3 . Results and Discussion. **11**, 207–211 (2008).

55. Baranauskaite, J. *et al.* Formation and investigation of electrospun Eudragit E100/oregano mats. *Molecules* **24**, 1–13 (2019).

56. Warnken, Z., Puppolo, M., Hughey, J., Duarte, I. & Jansen-Varnum, S. In Vitro–In Vivo Correlations of Carbamazepine Nanodispersions for Application in Formulation Development. *J. Pharm. Sci.* **107**, 453–465 (2018).

57. Lee, Y. H., Mei, F., Bai, M. Y., Zhao, S. & Chen, D. R. Release profile characteristics of biodegradable-polymer-coated drug particles fabricated by dual-capillary electrospray. *J. Control. Release* **145**, 58–65 (2010).

58. Pathak, S. *et al.* Preparation of high-payload, prolonged-release biodegradable poly(lactic-co-glycolic acid)-based tacrolimus microspheres using the single-jet electrospray method. *Chem. Pharm. Bull.* **64**, 171–178 (2016).

59. Yu, L. Amorphous pharmaceutical solids: Preparation, characterization and stabilization. *Adv. Drug Deliv. Rev.* **48**, 27–42 (2001).

60. Kong, L. & Ziegler, G. R. Role of molecular entanglements in starch fiber formation by electrospinning. *Biomacromolecules* **13**, 2247–2253 (2012).

61. Kong, L. & Ziegler, G. R. Rheological aspects in fabricating pullulan fibers by electro-wet-spinning. *Food Hydrocoll.* **38**, 220–226 (2014).

62. Klossner, R. R., Queen, H. A., Coughlin, A. J. & Krause, W. E. Correlation of Chitosan's rheological properties and its ability to electrospin. *Biomacromolecules* **9**, 2947–2953 (2008).

63. Skrdla, P. J., Floyd, P. D. & Dell'Orco, P. C. Predicted amorphous solubility and dissolution rate advantages following moisture sorption: Case studies of indomethacin and felodipine. *Int. J. Pharm.* **555**, 100–108 (2019).

64. Nevitt, S. J., Marson, A. G. & Smith, C. T. Carbamazepine versus phenytoin monotherapy for epilepsy: An individual participant data review. *Cochrane Database Syst. Rev.* **2019**, (2019).

Appendix
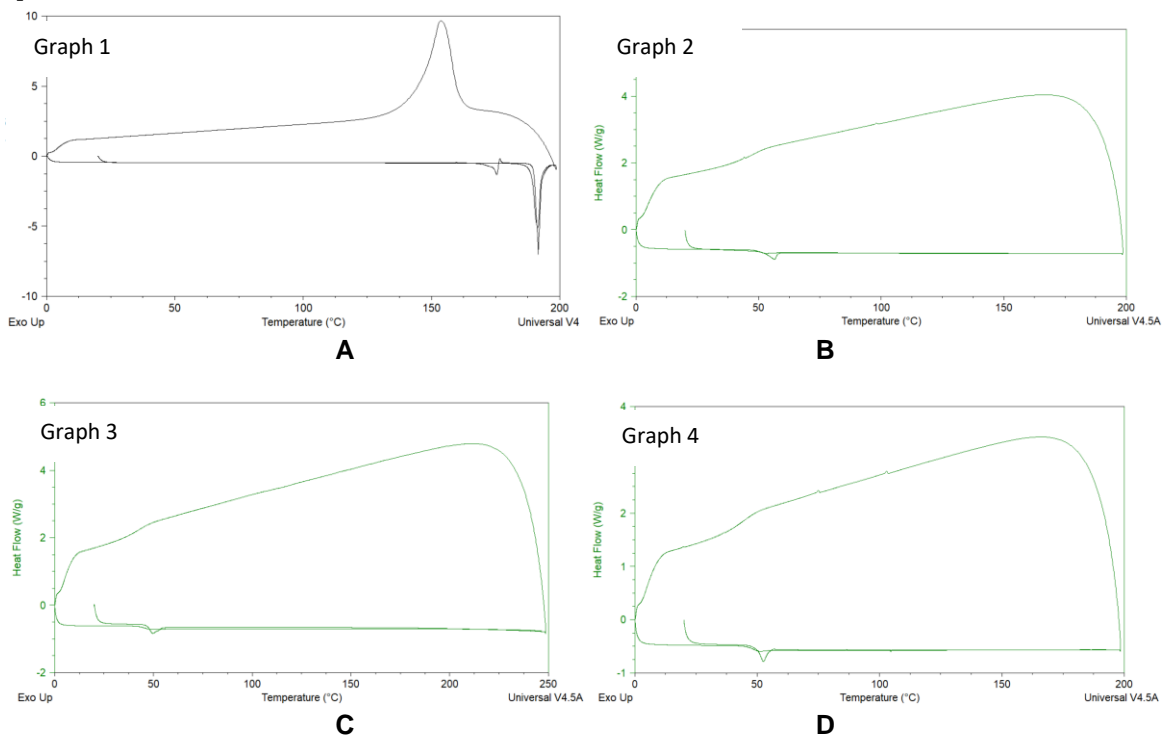
Figure S1 - DSC thermographs of A): Carbamazepine, B): PLGA 75-115kDa, C): PLGA 90kDa and D): PLGA 154kDa.
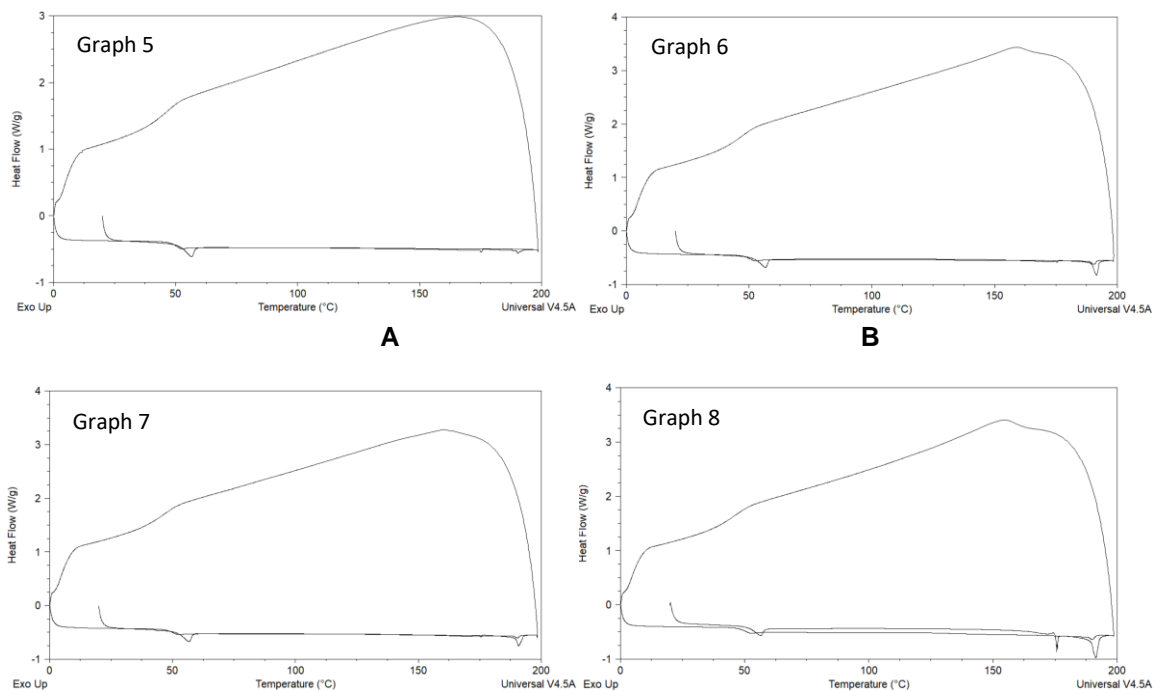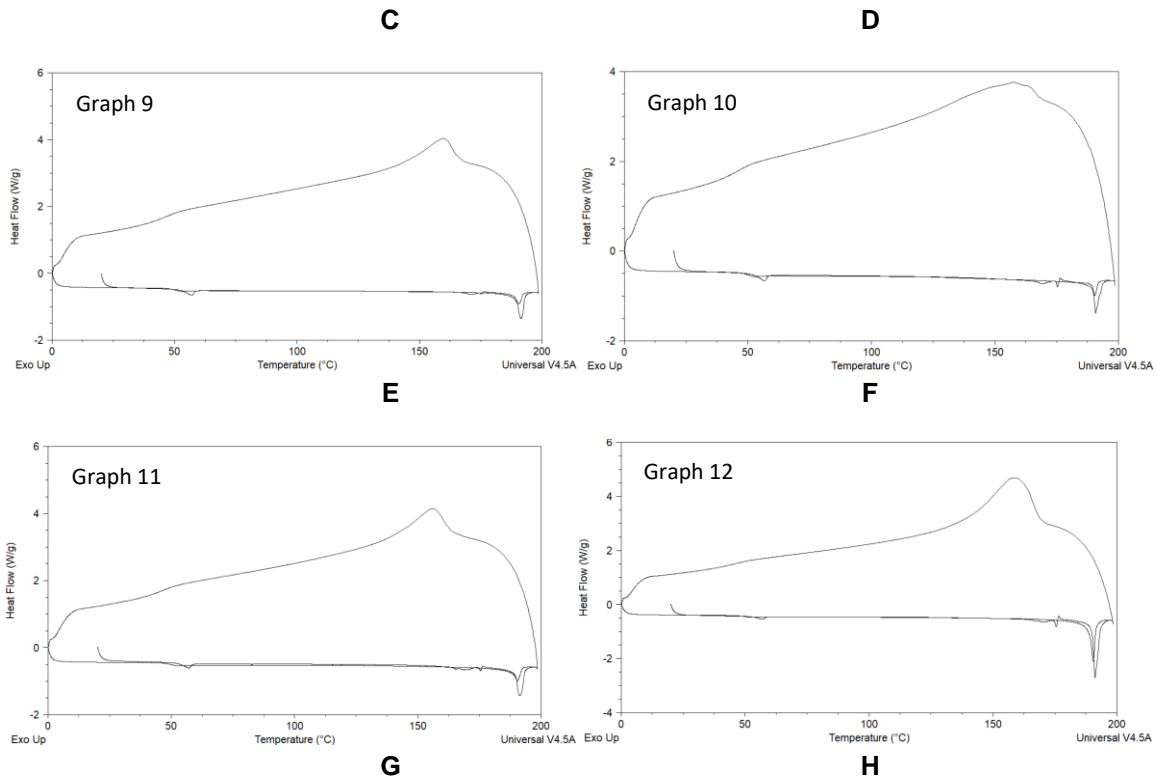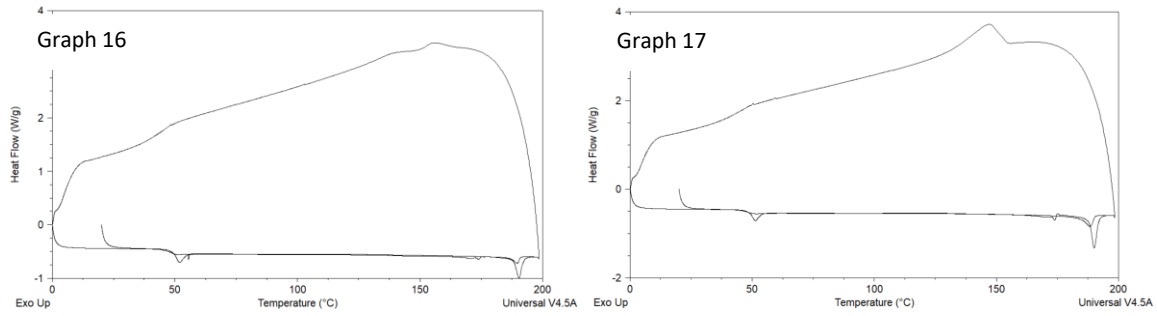
Figure S2- DSC thermographs of A): 9% Carbamazepine in PLGA 75-115kDa, B): 11% Carbamazepine in PLGA 75-115kDa, C): 12.5% Carbamazepine in PLGA 75-115kDa D): 15% Carbamazepine in PLGA 75-115kDa, E): 20% Carbamazepine in PLGA 75-115kDa, F): 25.7% Carbamazepine in PLGA 75-115kDa, G): 30% Carbamazepine in PLGA 75-115kDa and H): 50% Carbamazepine in PLGA 75-115kDa.
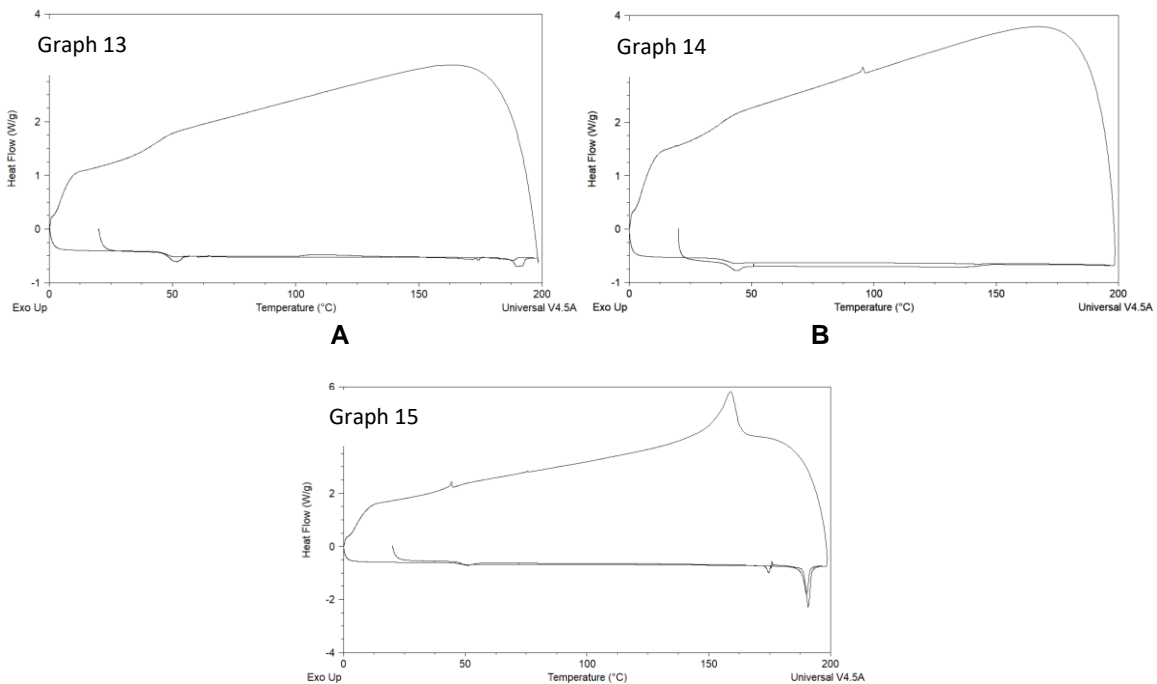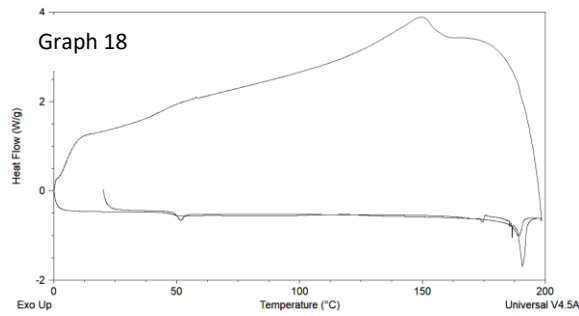
C

Fig. S3 - DSC thermographs of A): 11% Carbamazepine in PLGA 90kDa, B): 20% Carbamazepine in PLGA 90kDa, C): 30% Carbamazepine in PLGA 90KDa.
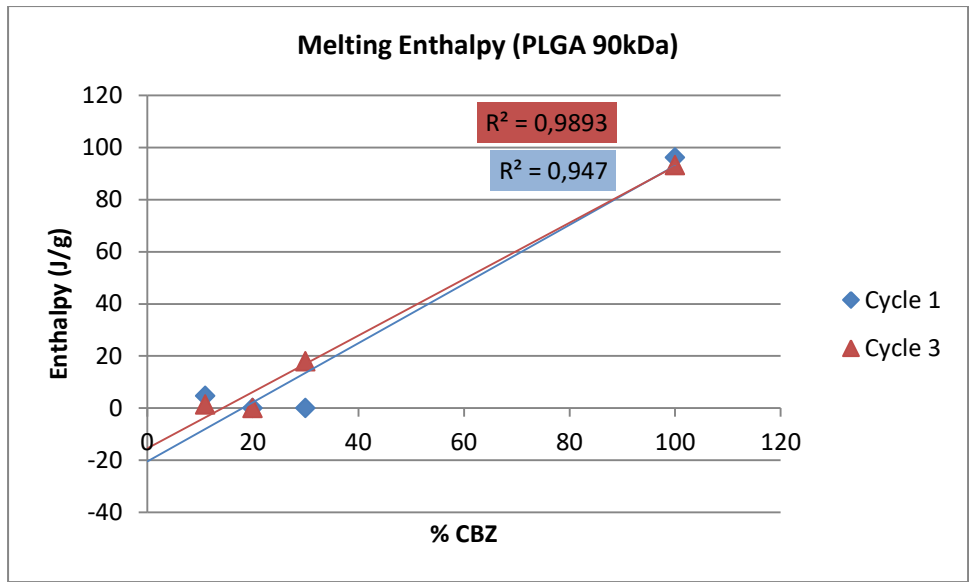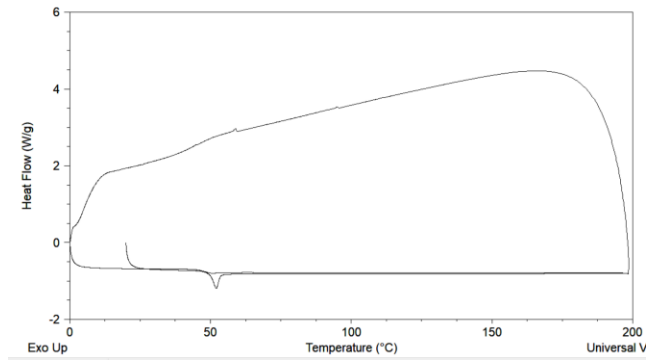

A

B

C

Figure S4 - DSC thermographs of A): 11% Carbamazepine in PLGA 154kDa, B): 20% Carbamazepine in PLGA 154kDa, C): 30% Carbamazepine in PLGA 154KDa.

Figure S5- Plot of Melting Enthalpy of CBZ as a function of CBZ concentration (cycles 1 and 3) – PLGA 90kDa physical mixtures

Figure S6 - DSC thermographs of electrospun fibres of PLGA 154kDa.